UNIVERSITYOF BIRMINGHAM

Acoustic emission study of fatigue crack propagation in extruded AZ31 magnesium alloy

Han, Zhiyuan ; Luo, Hongyun ; Sun, Chuankai; Papaelias, Mayorkinos; Davis, Claire

[Link to publication on Research at Birmingham portal](#)

Acoustic emission study of fatigue crack propagation in extruded AZ31 magnesium alloy

Zhiyuan Han[a], Hongyun Luo[a*], Chuankai Sun[a], Junrong Li[a], Mayorkinos Papaelias[b], Claire Davis[b]

a Key Laboratory of Aerospace Advanced Materials and Performance, Ministry of Education

School of Materials Science and Engineering, Beihang University

Beijing, China

b   School of Metallurgy and Materials, University of Birmingham,

Birmingham, United Kingdom

***E mail:** luo7128@163.com **Fax: Tel:** 0086-010-82339905

Address: 8th Lab of the School of Material Science and Engineering, Beijing University

of Aeronautics and Astronautics, No.37 Xueyuan Road, Haidian District, Beijing, People's

Republic of China, 100083

Abstract

The fatigue crack propagation behaviour and corresponding AE characteristics of extruded AZ31 magnesium (Mg) alloy were investigated in this study. The effects of specimen orientation and loading frequency were considered. By combining the AE parameter and waveform analysis with the micro-structural and fractograph observations, the findings of the study showed that crack extension and twinning at the crack tip were two major AE source mechanisms during fatigue crack propagation of Mg alloy. More twinning events were observed in transverse direction specimens than that in extruded direction specimens, which contributed to more cyclic deformation irreversibility and cumulative fatigue damage, leading to worse fatigue

performance and higher AE counts in TD specimens. The results also indicated that increasing the loading frequency could slightly increase the fatigue life, and significantly decrease the AE counts in transverse direction specimens due to the frequency or strain rate dependence of twinning activity. These results suggest that twinning play an important role in fatigue process of Mg alloy, and AE technique is capable of detecting crack propagation and twinning events during fatigue.

1 Introduction

Magnesium (Mg) alloys are very attractive as structural materials in automotive and aerospace applications due to the significant advantages they offer. such as high strength-to-weight ratio, high specific stiffness and high thermal conductivity. For the applications as load-bearing components in service, the fatigue properties of Mg alloys are of great importance, because they always involve cyclic loads and deformation, thus it is necessary to understand their fatigue crack propagation (FCP) behaviour and mechanisms for safety reason. Previous studies focusing on the low cycle fatigue of Mg alloys indicated that the interactions between dislocation slip, twinning, and de-twinning processes played important roles in their cyclic deformation behaviour [1,2]. Furthermore, it is showed that the fatigue crack nucleation and growth during high cycle fatigue process were also controlled by these

mechanisms. For example, Ochi et al. and Yang et al. suggested that twin boundaries could act as preferential sites for crack nucleation [3, 4], and Zeng et al. indicated the similar role for slip bands near particles [5]. Understanding the roles of these mechanisms during FCP is of great importance for improving the fatigue properties of Mg alloys.

On the other hand, the FCP process of Mg alloys can be influenced by many factors. It is well known that the slip and twinning during deformation process in hexagonal close packed (HCP) structure Mg alloys are influenced by the crystal orientation. Thus the fatigue properties are strongly dependent on the texture of material and orientation of specimen. In wrought Mg alloys which have strong texture anisotropic behaviour is exhibited [6-8]. The loading frequency is another important factor can influence the FCP behaviour of Mg alloys. Generally the increasing frequency led to increase of fatigue life and decrease of fatigue growth rate in air environment, however the governing mechanism is still controversial and needs further investigation.. The environment-assisted cracking behaviour, crack closure behaviour, oxide films formed on the fracture surface, and strain rate during FCP can be all influenced by the frequency and result in different fatigue properties [9-11]. In addition, there is currently limited literature which reports the effects of frequency in different orientations of wrought Mg alloys with texture. The influence and the corresponding mechanisms of these factors still need further investigation.

Acoustic emission (AE) is widely used as a structural health monitoring technique to detect deformation, fracture and phase transition process in a variety of materials. The continuous monitoring of FCP process is one of the applications of AE, which has been widely investigated in metal alloys, especially in steels and aluminum alloys [12-14]. The advantage of AE is the in-situ analysis of the micro-damage events. Many previous AE studies focused on the tension process of Mg alloys, and showed that the AE technique could successfully capture and identify the slip and twinning events during deformation [15-17]. However, according to author's knowledge, there have been very few studies on the AE during fatigue process of Mg alloys. The AE source mechanisms and the influence of specimen orientation and frequency on AE during FCP are still unclear. Thus this study is an attempt to study AE behaviour during the FCP process of an extruded AZ31 alloy, and investigate the influence of specimen orientation and frequency on FCP and AE characteristics.

2. Experimental details

Commercial extruded AZ31 (nominal composition Mg + 3wt.% Al + 1wt.% Zn) Mg alloy sheet was used in this study. The average grain size of the material is about 20 μm, as shown in Fig. 1a. The texture of the material was examined by electron backscatter diffraction (EBSD) method, and the pole figures of (0002), (11-20), and (10-10) are shown in Fig. 1b. It can be seen that the basal (0001) planes are parallel to the extrusion direction (ED) and perpendicular to transverse direction (TD), which is common for extruded AZ31 alloys [6, 18]. Two types of standard compact tension

(CT) specimens were prepared with loading axis parallel (ED specimens) and perpendicular (TD specimens) to the ED. The shape and dimensions of compact tension (CT) specimens were shown in Fig. 1c. Standard tensile tests were also performed with flat specimens for ED and TD orientations to obtain the tensile properties.

Fatigue tests were carried out on an Instron 8801 servo-hydraulic testing machine at ambient temperature (300 K). Specimens were tested under sinusoidal cyclic loading at three frequency levels of 2Hz, 10Hz, and 20Hz. The load ratio R employed was 0.1. The peak load was 3kN for both ED and TD specimens. At least three specimens were tested under each condition to confirm the regularity. The fatigue crack length was measured by a standard crack tip opening displacement (CTOD) gage, which had an accuracy of 0.01 mm and was set at the tip of the initial notch. The crack length data of each cycle was recorded, and the stress intensity factor range ΔK was calculated from the crack length simultaneously.After the fatigue tests, the fracture surfaces were observed using scanning electron microscope (SEM, Model: JSM-5800, JEOL, Japan).

AE signals generated during the fatigue tests were recorded and analysed by using a DiSP data acquisition card with AEwin v2.19 acoustic emission system (Physical Acoustic Corporation, USA). Two piezoelectric transducers (R15) with a bandpass filter from 100kHz to 400kHz and a resonant frequency of 150 kHz were used to pick

up AE signals with a preamplifier with 40 dB gain. The sensors were attached to the specimen with tape. Vaseline was used at the interface between the sensors and the specimen surface to detect the AE activity. The positions of AE sensors are shown in Figure 1c. A compatible amplitude threshold of 40dB and a average frequency threshold of 35kHz were used in the experiment to filter the background noise. Considering that the crack propagation and fracture events can only occur at higher loads, a load threshold of 2.55kN (85% maximum load) was used to eliminate fixturing and crack closure noise at lower loads.
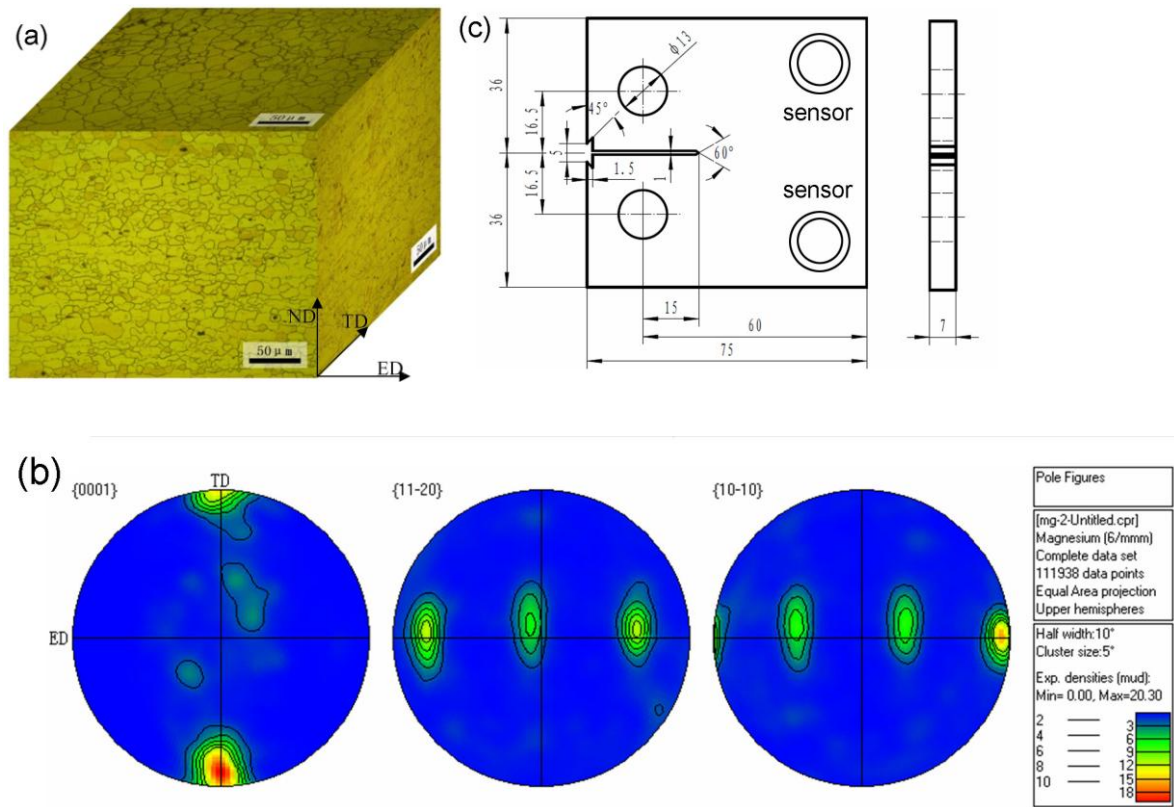

Fig. 1 (a) Optical observations of micro-structures, (b) pole figures of (0002), (11-20), and (10-10) for the extruded AZ31 alloy. (c) Details of the CT specimen

3 Results and discussion

3.1 Tensile properties

The engineering stress-strain curves for ED and TD orientations are shown in Fig 2. It can be seen that the yield strength is about 180MPa in ED specimen, nearly twice that in TD specimen. This strong anisotropy in tensile properties is related to the different deformation mechanisms and texture in material [19]. It is well known that the {10-12}<-1011> tension twin can be activated to accommodate extensions along c axis of the hexagonal lattice. Compared with the slip deformation mode in ED specimen, the twinning is a more favorable plastic deformation mechanism in TD specimen, whose loading direction is parallel to c axis. Thus, the lower strength for TD specimens can be explained by the lower critical shear stress (CRSS) for twinning than that for prismatic and pyramidal slip in hcp Mg alloy at room temperature as reported in Equation (20) of the Ref [20]. These results were confirmed by micro-structure observation and are consistent with previous studies [19].
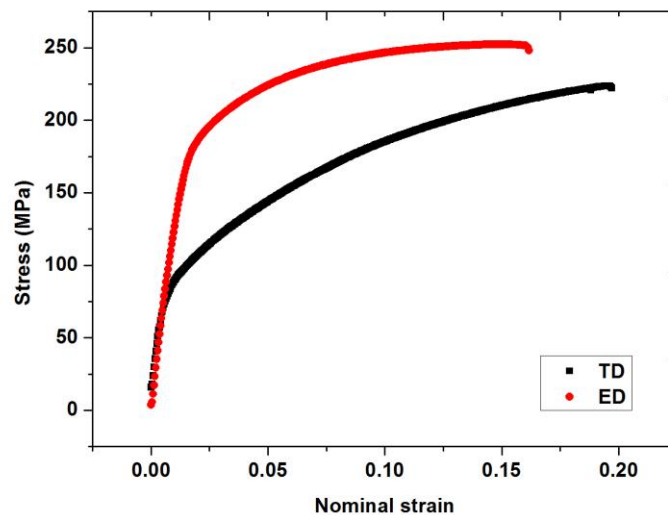

Fig. 2 Stress - strain curves during tensile tests for ED and TD specimens

Table 1 Yielding and tensile strength, fatigue life, and experimental constants of FCP and

AE count rates for different specimens

Specimens	Yield strength (MPa)	Tensile strength (MPa)	Number of cycles	m	logD	P	logB
ED-3kN-2Hz			40295	2.22	-5.54	8.45	-8.40
ED-3kN-10Hz	180	260	36267	2.93	-6.34	8.08	-7.80
ED-3kN-20Hz			33248	2.88	-6.27	8.02	-7.98
TD-3kN-2Hz			33009	2.85	-6.12	3.20	-1.38
TD-3kN-10Hz	80	230	29810	2.89	-6.19	3.57	-2.07
TD-3kN-20Hz			28396	2.97	-6.37	3.37	-2.08

3.2 Fatigue properties

3.2.1 Fatigue life and FCP rate results

The anisotropy is also observed in fatigue behaviour during cyclic deformation. Fig. 2b shows the crack lengths versus the number of loading cycles for ED and TD specimens with different frequency. The fatigue life of ED specimens was always longer than that of TD specimens at the same loading frequency as shown in Fig. 3a, which suggests the better fatigue resistance in ED specimens. The evidently higher FCP rates observed in TD specimens than ED specimens at higher ΔK level also support this result as indicated in Fig. 3b. While at lower ΔK, the differences in FCP rates between ED and TD specimens were found to be minimal. In this stable FCP stage (Paris regime), the relationships between the FCP rates (da/dN) and stress intensity factor ranges (ΔK) for all specimens follow the Paris–Erdogan Equation [21]:

$$\frac{da}{dN} = D\Delta K^m, \ or: \ \log(\frac{da}{dN}) = \log D + m \log \Delta K \tag{1}$$

The material constants D and m for different specimens as summarized in Table 1 also show the similar values between ED and TD specimens. It is noteworthy that though the higher frequency led to a slight increase of fatigue life (Fig 3a), little loading frequency dependence of FCP rate was observed for both ED and TD specimens.
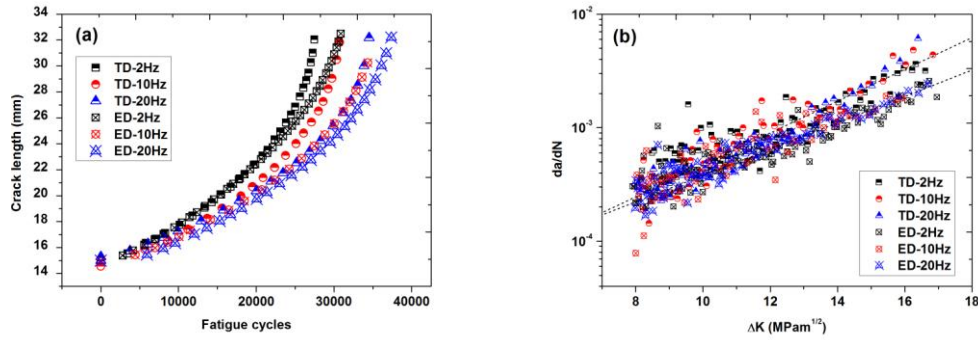
Fig. 3 (a) Crack lengths versus numbers of fatigue cycles, and (b) relationships between crack growth rates and ΔK for different specimens

3.2.2 Influence of specimen orientation on fatigue properties

The longer fatigue life observed in ED specimens than TD specimens for extruded AZ31 alloy in the present study is consistent with the results reported in a previous study by Ishihara et al. [6]. This can be also expected from the tensile properties, because the fatigue strength usually increases with the yield strength for metals. However, comparing with the strong anisotropy in yield strength, the differences in fatigue lives and FCP rates are relatively small between ED and TD specimens, especially at lower ΔK. It implies that at lower ΔK level, the significant difference in plastic deformation mechanisms (slip and twinning) for different orientations may

have little influence on FCP behaviour. It can be attributed to the fact that the plastic deformation is very limited at the tip of the crack during FCP at lower ΔK, which is supported by two experimental observations: Firstly, the fractograph of the fatigued ED and TD specimens displayed the similar characteristics of flat and cleavage-like facets as shown in Fig. 4a and b, which can be also observed throughout the whole fracture surfaces regardless of the loading frequency. It suggests that the fatigue fracture of AZ31 alloy were essentially brittle rather than ductile. The cleavage fracture of the Mg alloy was also well reported in literatures [22-25], and Reed et al. demonstrated that the cleavage fracture in Mg single crystal is not observed on prismatic planes or in {10-12} tension twins [22]. Secondly, the optical observations of the cross-sectional micro-structures near fracture surface in Fig 5a and b reveal that relatively low amount of twins were generated at lower ΔK in both specimens (compared with that at higher ΔK in Fig 5c and d), also suggesting the plastic deformation is limited at lower ΔK. Thus, the FCP behaviour can be expected to be independent of plastic deformation at lower ΔK level.

However, the plastic deformation may play more and more important roles when the crack increases in size. It is believed that the differences in FCP rates between ED and TD specimens (Fig. 3b) at higher ΔK are due to the twinning-involved fatigue damage process. By comparing Fig. 5a and b with Fig. 5c and d, it can be seen that more twins were generated near crack tip at higher ΔK level. These twins are mainly {10-12} tension twins induced by cyclic tension stress along c-axis during fatigue. The

nucleation and growth of tensile twinning system induced by mode I crack propagation in Mg alloy were also well discussed and simulated by phase-field analysis by Clayton et. al. recently [26]. Thus similar to the tensile results, more considerable twins can be observed in TD specimens than ED specimens. Ochi et al. and Yang et al. indicated that the twinning involved cyclic deformation irreversibility and the twin boundaries could promote the fatigue crack nucleation and growth [3, 4]. Thus the higher FCP rates of TD specimens can be explained by their much higher twin fractions at the crack tip compared to ED specimens.
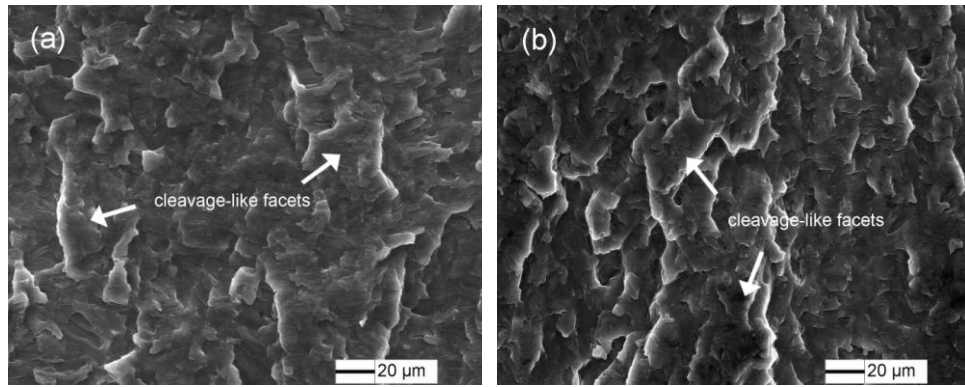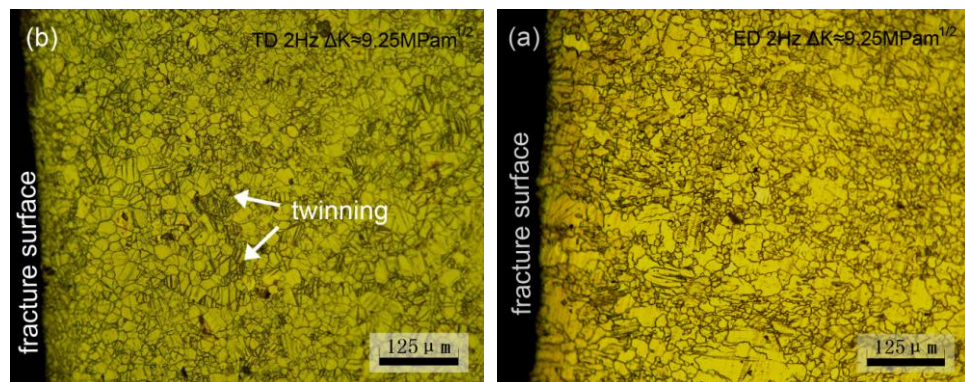

Fig. 4 Scanning electron micrographs of fracture surfaces for (a) ED and (b) TD specimens at ΔK about 12 MPam$^{1/2}$ (at frequency of 10Hz)
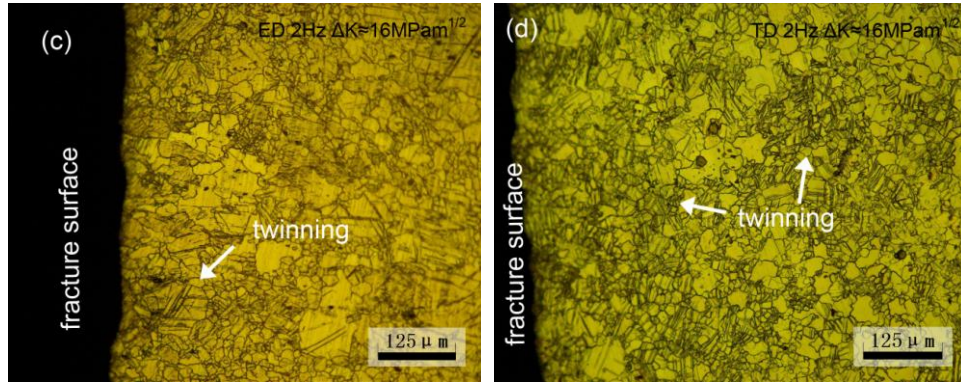
Fig. 5 Optical observations of the cross-sectional micro-structures near fracture surface for (a, c) ED and (b, d) TD specimens at ΔK about (a, b) 9.25 MPam$^{1/2}$ and (c, d) 16 MPam$^{1/2}$ (at frequency of 2Hz)

3.2.3 Influence of frequency on fatigue properties

Decreasing frequency usually decreases the fatigue life in Mg alloys at air environment, which is in consistent with the present results. The reason can be attributed to the more severe hydrogen embrittlement, stress corrosion cracking, and also the oxide film micro-cracking at lower frequency due to the longer reaction time [9-10]. However, in contrast, Rozali et al. indicated that the decreasing frequency might decrease the FCP rate due to the crack closure behaviour in NaCl environment [11]. Zeng et al. also discussed the influence of strain rate on FCP at different frequency [27]. In the present study, the influence of frequency on fatigue life, and especially on FCP rate, is not significant in both orientations as shown in Fig. 3b. It suggests that the above factors may all play a role during FCP, which leading to a complicated influence of frequency on FCP behaviour.

3.3 AE characteristics

3.3.1 AE count and count rate results

The AE count was used to analyse the AE behaviour during FCP in this study. The cumulative AE counts versus fatigue cycles and the total AE counts for different specimens are represented in Fig. 6a and b respectively. The interesting observation is that much higher AE counts were generated in TD specimens than ED specimens at the same frequency level. It can be also observed that an increasing frequency led to a significant increase in AE counts for TD specimens, but this increase was very limited for ED specimens. Fig. 7a shows the relationships between AE count rates (dC/dN) and ∆K, which can be expressed by an equation similar to the Pairs law for all specimens [28]:

$$\frac{dC}{dN} = B\Delta K^p \text{, or: } \log(\frac{dC}{dN}) = \log B + p \log \Delta K \tag{2}$$

The parameter B and p for different specimens are summarized in Table 1. It can be seen that the dC/dN is much higher in TD specimens and at lower frequency, and the influence of frequency is also much more significant in TD specimens than in ED specimens, which are in agreement with the AE count results.
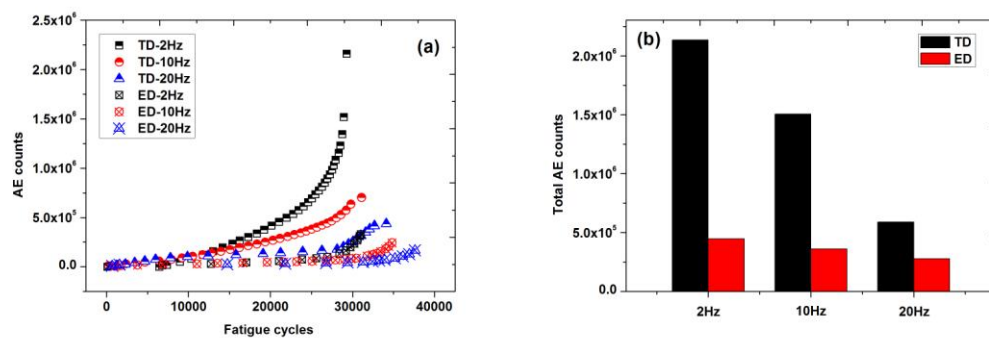

Fig. 6 (a) Cumulative AE counts versus fatigue cycles; (b) total AE counts (average of three
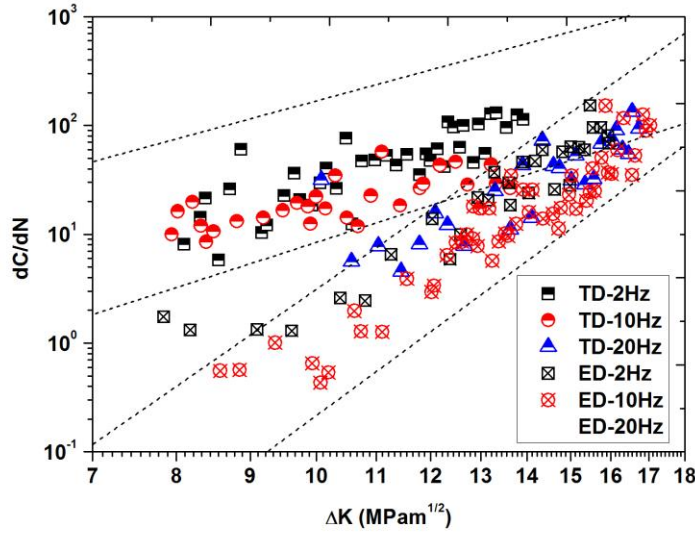
Fig. 7 Relationships between AE count rates and ΔK

3.3.2 AE source mechanisms and influence of specimen orientation on AE

To reveal the influence of specimen orientation and frequency on AE behaviour, it is essential to understand the AE source mechanisms during FCP in Mg alloy. It is reported that the cyclic plasticity ahead of the crack tip activity and the crack tip micro-fracture are primary AE source mechanisms during FCP for ductile and brittle materials respectively [29]. The fractograph in Fig. 4 has demonstrated the brittle fracture characteristics during fatigue of AZ31 alloy in the present study, thus the energy released from the crack extension could be considered as a detectable AE source. However, only this mechanism can't explain the difference in AE counts and count rates between different specimens. Fig. 8 shows the relationships between dC/dN and da/dN, the higher dC/dN for TD specimens than ED specimens and the decreasing dC/dN with frequency at the same da/dN suggest that the AE generated per unit crack length is higher in TD specimens and at lower frequency. It indicates

that the different AE counts and count rates for different specimens should be attributed to other mechanisms rather than the difference in FCP rates.
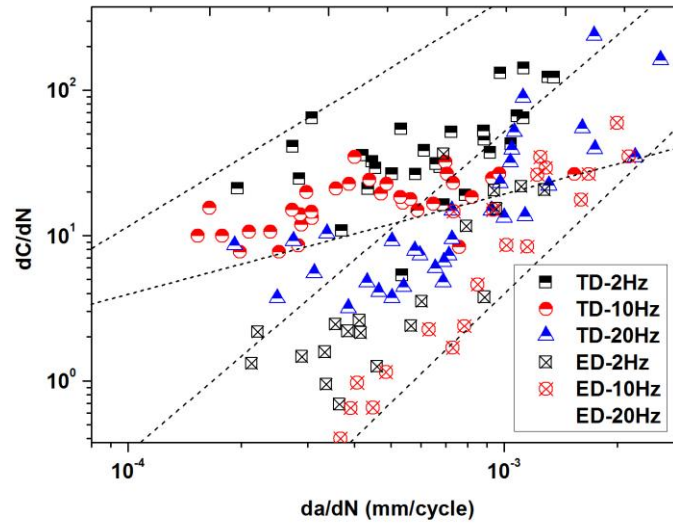
Fig. 8 Relationships between AE count rates and FCP rates for different specimens

The twinning events ahead of the crack tip are suggested to be another important AE source mechanism during FCP of AZ31 alloys. This mechanism has been widely demonstrated in tensile, compression, and cyclic deformation in Mg alloys [15-17, 30]. Though it was discussed that the plasticity was not the major AE source mechanism in brittle fractured materials and was limited at lower ΔK in present study, it is believed that the twinning events can be still detected by AE during FCP considering that the twinning is a relatively intense AE source compared to dislocation slip [15-17]. This mechanism is also strongly supported by the results of higher AE counts and count rates in TD specimens than ED specimens (Fig. 6 and Fig. 7), because more AE activity would be generated due to the higher amount of twins in plastic zone of TD specimens (Fig. 5).

To further verify and identify these two AE source mechanisms, a multi-parametric analysis of rise time (*RT*) versus amplitude (*Amp*) was performed at different ΔK ranges (lower ΔK range before 10MPam$^{1/2}$ and higher ΔK range after 14MPam$^{1/2}$) for ED and TD specimens, the typical results are shown in Fig. 9. In the case of ED specimens, it can be seen that most AE signals display a *RT* distribution within 200μs and an *Amp* distribution from 40 to 80dB at lower ΔK range (Fig. 9a). However, a large number of AE signals with *RT* higher than 200μs (*Amp* ranges from 45 -75 dB) are observed at higher ΔK level. The similar characteristics for AE signals are also observed in TD specimens as shown in Fig. 9b, except that much higher *RT* (>200μs) signals are generated in both lower and higher ΔK ranges.

It is reported that the *Amp* and *RT* distributions of AE signals can reflect the AE source characteristics, and signals with *Amp* and *RT* distributions from 40-50dB and 0-200μs were related to dislocation activity ahead of the crack during FCP in steels by Han et al [31]. In the present study, the signals with higher *RT* (>200μs) and *Amp* (45-75dB) is assumed to be generated from twinning events, because these signals are fewer in ED specimens at lower ΔK range and much more significant in TD specimens, which is well consistent with their different twin fractions as shown in Fig. 5. In addition, the typical waveform and corresponding Fast Fourier Transformed (FFT) spectrum for these signals are shown in Fig. 10a, and compared with those for signals from the yielding stage during tensile test of TD specimens in Fig. 10b, which

is supposed to be the plastic events related to twinning as discussed in section 3.1. It can be seen that both signals are composed of several burst type waveforms and also contain some continuous components. The similarity in waveform and spectrum between these two types of signals also indicates that the twinning is a responsible mechanism for the signals during fatigue. On the other hand, the signals with lower *RT* (<200μs) can be considered to be the crack extension events, thus exhibiting the similar characteristics in both TD and ED specimens and at different ΔK ranges as seen in Fig 9. The AE waveform and spectrum for these signals in Fig. 10c show a typical burst type waveform, which is usually the fingerprint for crack propagation events, and poor frequency matching between that in Fig. 10a and b. Furthermore, these signals show the higher *Amp* distributions (40-80dB) than that in steel (40-50dB), which also implies that they are generated from a more intense source such as crack extension rather than dislocation activity [31].
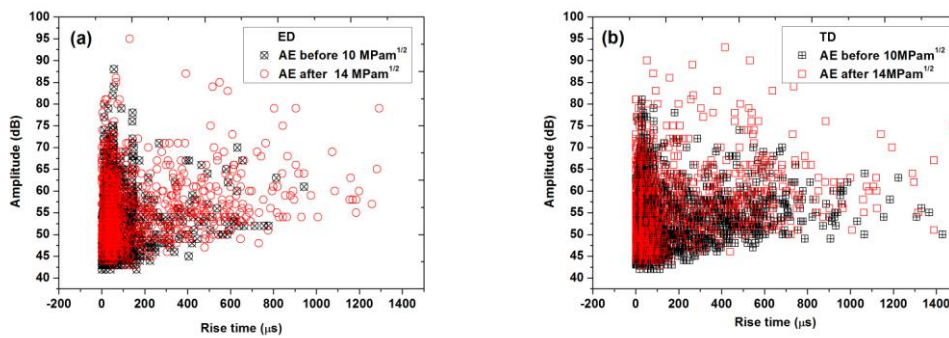
Fig. 9 Amplitude versus rise time at different ΔK ranges for (a) ED and (b) TD specimens
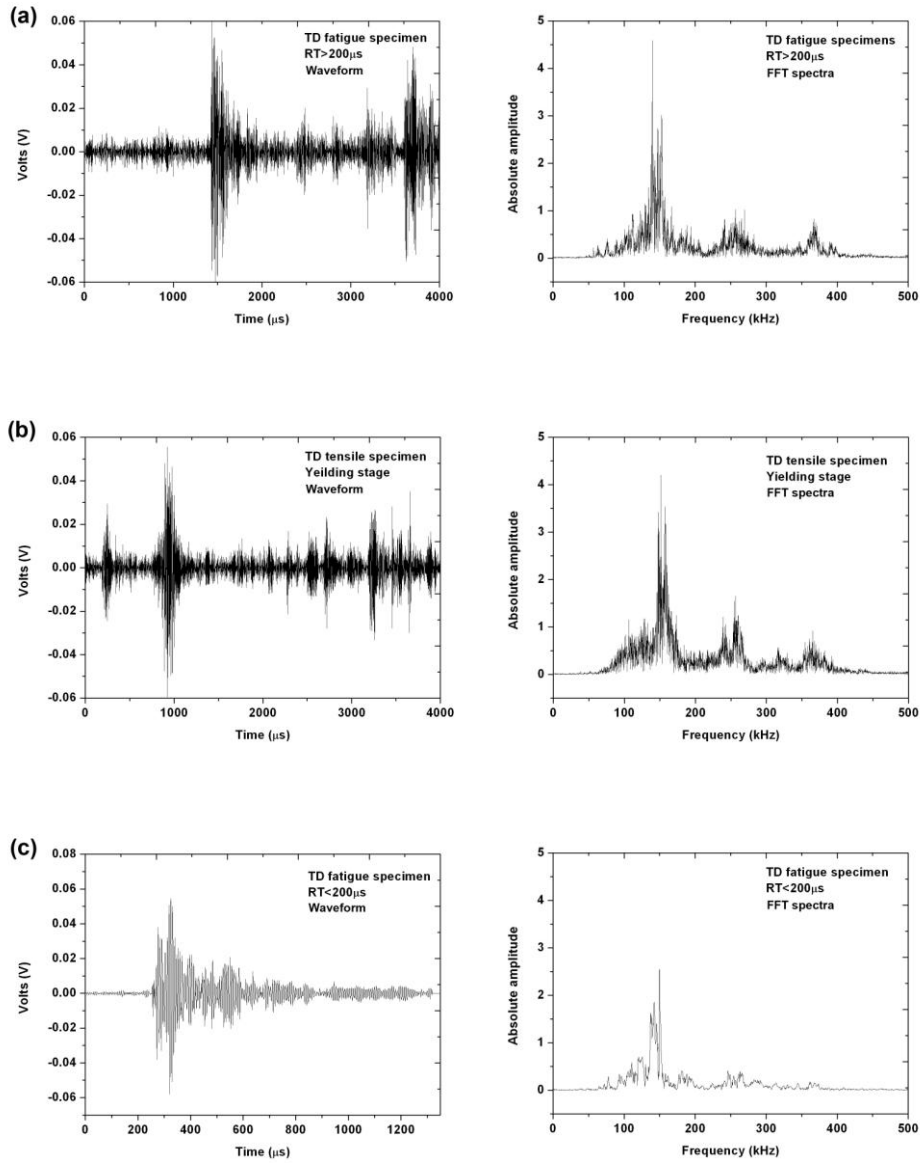
Fig. 10 Typical waveforms and FFT spectrum for (a) signals with higher RT (>200μs) during fatigue test for TD specimen (b) signals in yielding stage during tensile test for TD specimen (c) signals with lower RT (<200μs) during fatigue test for TD specimen

Based on the above analysis, a rough clustering of twinning events and crack extension events can be made according to their different *RT* distributions, which are *RT* <200μs and *RT* >200μs respectively. A calculation of the cumulative AE counts

for these two groups of signals is performed for ED and TD specimens and the results

are shown in Fig. 11. It shows that the cumulative AE counts corresponding to

twinning events (RT >200μs) are much higher in TD specimens than that in ED

specimens. These signals contribute a major proportion of AE activity during FCP in

TD specimens, but only a few in ED specimens, which is consistent with their

different twin fractions (Fig. 5). However, for the crack extension events (RT <200μs),

the AE counts is similar between ED and TD specimens, this result is also well in

agreement with their similar fracture mode (Fig. 4) and FCP rates (Fig. 3b). The

higher AE counts for crack extension events in TD specimens may be attributed to

their higher FCP rates and the rough clustering of two groups. Again, these results

support that the twinning and crack extension are two major AE source mechanisms

during FCP of AZ31 alloys, more accurate signal categorization analysis [15, 32] may

be needed in future work to further identify these two mechanisms during FCP.
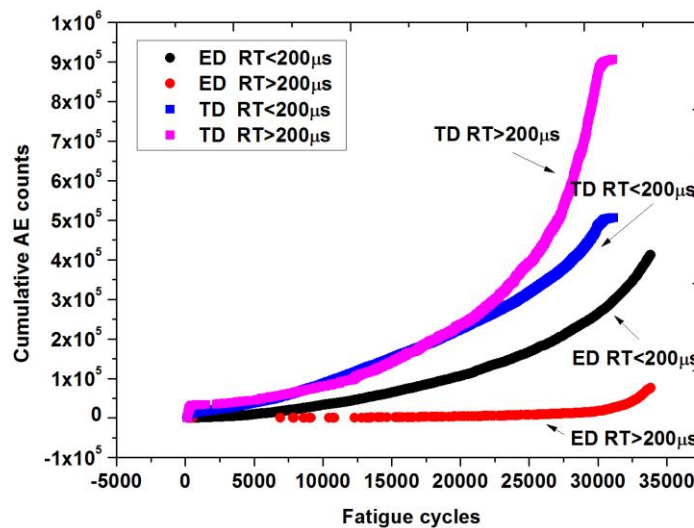

Fig. 11 Cumulative AE counts for AE events with *RT* <200μs and *RT* >200μs in ED and TD

speciemns during FCP

3.3.3 Influence of frequency on AE

The relatively different effects of frequency on AE between ED and TD specimens can be also attributed to their different twinning activity and the corresponding frequency dependence. Other mechanisms, for example environment-assisted cracking behaviour, crack closure behaviour, oxide films formed on the fracture surface can be excluded as the causes of the frequency effects during FCP, because if these mechanisms are responsible for the higher AE activity at lower frequency in TD specimens, the similar frequency dependence of AE is also expected in ED specimens due to the similar FCP rates, which is different from the results in Fig. 6. Likewise, the effect of time-related noise from machine and friction can be also excluded.

It is known that the deformation twinning of Mg alloys is a strain rate dependent process, and the strain rate of the material ahead of the crack during FCP is related to the cyclic loading frequency as [33]:

$$\varepsilon'(t) = \pi f \frac{\sigma_{\max}}{E}(1-R)\cos(2\pi ft) \tag{3}$$

$$\varepsilon'_{\max} = \pi \frac{\sigma_{\max}}{E}(1-R)f \tag{4}$$

where $\varepsilon'(t)$ and $\varepsilon'_{\max}$ are the strain rate and maximum strain rate, R, f and t are stress ratio, frequency and time, respectively, and $\sigma_{\max}$ is the maximum tensile stress. Equation 3 and 4 clearly demonstrate that the higher frequency will lead to the higher strain rate ahead of the crack during FCP, which generally increases the twinning activity during tensile deformation and also during fatigue in Mg alloys [19, 33-34].

However, Zeng et al. suggested that an excessive high strain rate may result in an opposite result because the twinning is difficult to take place due to the intense strain hardening at higher strain rate [5, 33]. In the present study, the decreased AE counts at higher frequency in TD specimens suggested the actual results might be the later case if the twinning is responsible for this frequency effects on AE. A comparison of cross-sectional micro-structures near fracture surface between 2Hz and 20Hz TD specimens in Fig. 12 supports this point, it can be seen that the area of plastic zone related to twinning is decreased at higher frequency. These results suggest that the intense cyclic hardening induced by high strain rate may constrain the further deformation ahead of the crack in TD specimens, thus significantly decreased the twinning activity and corresponding AE signals at high frequency. But for ED specimens, which showed a relatively low amount of twins during FCP, the influence of frequency on AE could be very limited as the results shown in Fig. 6 and Fig. 7.
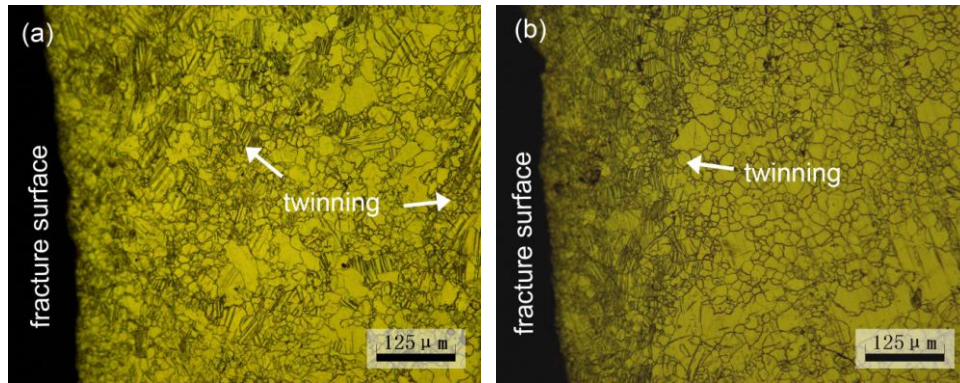

Fig. 12 Optical observations of the cross-sectional micro-structures near fracture surface for TD specimens at frequency of (a) 2Hz and (b) 20Hz (at ΔK about 16 MPam$^{1/2}$)

Though the above explanation can well explain the different frequency dependence of

AE in TD and ED specimens, it is still arbitrary to conclude that the twinning activity will be decreased with the increasing frequency during FCP in TD specimens for extruded Mg alloy. Firstly, the strain hardening behaviour of Mg alloys is not only dependent on the strain rate, but also on the micro-structural features such as grain size. Softening can be also induced by twinning when strain rate increased in coarse grains and at lower strain rate ranges [5]. Secondly, though Fig. 5 shows a typical example for micro-structural comparison between different frequency, but not all specimens exhibited the same regularity. Some TD specimens at higher frequency also revealed considerable twins and plastic zone size near the crack tip. Thus, other reasons for the frequency dependence of AE during FCP of Mg alloys can still not be ignored. One assumption is that the twinning induced FCP may generate more intense AE signals at lower frequency due to the hydrogen embrittlement assistance, this might be a possible explanation for the present finding, but its validity is still questionable and need further investigations.

Conclusions

The fatigue and AE characteristics during FCP process of extruded AZ31 alloy were investigated in this study. The effects of specimen orientation and frequency were also discussed. The results show that AE technique is capable of acquiring crack propagation and plastic events during FCP of Mg alloy. The results obtained from the present study can be summarized as follows:

1. The fatigue life was longer for ED specimens than that for TD specimens. The

FCP rates were similar between ED and TD specimens at lower ΔK, but were higher in TD specimens than that in ED specimens at higher ΔK. More twinning was observed in TD specimens and at higher ΔK level, which contributed to more cyclic deformation irreversibility and cumulative fatigue damage, leading to worse fatigue performance in TD specimens.

2. Increasing frequency led to slight increase of fatigue life, but had limited influence on the FCP rates for both ED and TD specimens. Environment-assisted cracking behaviour, crack closure behaviour, and strain rate effects may all play a role during FCP, leading to a complicated influence of frequency on FCP bebaviors.

3. Crack extension and twinning at the crack tip were two major AE source mechanisms during FCP process of AZ31 alloy. These two mechanisms showed different waveforms and *RT - Amp* distributions, which can be used to identify these two mechanisms during FCP.

4. The AE counts and count rates were much higher in TD specimens than that in ED specimens due to the more twinning events in TD specimens during fatigue.

5. The increasing frequency significantly decreased AE counts and counts rates in TD specimens, but had limited influence in ED specimens, which can be attributed to their different twinning activity and the corresponding frequency or strain rate dependence. Cyclic hardening induced by high strain rate may constrain the further deformation ahead of the crack in TD specimens, thus decreased the twinning activity and AE signals at high frequency.

References:

[1] L. Wu, A. Jain, D.W. Brown, G.M. Stoica, S.R. Agnew, B. Clausen, D.E. Fielden, P.K. Liaw, Acta Mater. 56 (2008) 688–695.

[2] S.H. Park, S.G. Hong, W. Bang, C. S. Lee, Mater. Sci. Eng. A. 527 (2010) 417–423

[3] Y. Ochi, K. Masaki, T. Hirasawa, X. Wu, T. Matsumura, Y. Takigawa, K. Higashi, Mater. Trans. 47 (2006) 989–994.

[4] F. Yang, S.M. Yin, S.X. Li, Z.F. Zhang, Mater. Sci. Eng. A. 491 (2008) 131–136.

[5] R. Zeng, E. Han, W. Ke, W. Dietzel, K.U. Kainer, A. Atrens, Int. J. Fatigue 32 (2010) 411–419

[6] S. Ishihara, S. Taneguchi, H. Shibata, T. Goshima, A. Saiki, Int. J. Fatigue 50 (2013) 94–100.

[7] F. Lv, F. Yang, Q.Q. Duan, Y.S. Yang, S.D. Wu, S.X. Li, Z.F. Zhang, Int. J. Fatigue 33 (2011) 672–682.

[8] S. Morita, N. Ohno, F. Tamai, Y. Kawakami, Trans. Nonferrous Met. Soc. China 20 (2010) 523−526.

[9] Y. Kobayashi, T. Shibusawa, K. Ishikawa, Mater. Sci. Eng. A. 234-236 (1997) 220-222.

[10] K. Tokaji, M. Nakajima, Y. Uematsu, Int. J. Fatigue 31 (2009) 1137–1143.

[11] S. Rozali, Y. Mutoh, K. Nagata, Mater. Sci. Eng. A. 528 (2011) 2509–2516.

[12] T.M. Roberts, M. Talebzadeh, J. Constr. Steel. Res. 59 (2003) 679–694.

[13] Z. Han, H. Luo, J. Cao, H. Wang, Mater. Sci. Eng. A. 528 (2011) 7751–7756.

[14] H. Chang, E.H. Han, J.Q. Wang, W. Ke, Int. J. Fatigue 31 (2009) 403–407.

[15] A. Vinogradov, D. Orlov, A. Danyuk, Y. Estrin, Acta Mater. 61 (2013) 2044–2056.

[16] O. Muránsky, M.R. Barnett, D.G. Carr, S.C. Vogel, E.C. Oliver, Acta Mater. 58 (2010) 1503–1517.

[17] K. Máthis, F. Chmelík, M. Janeček, B. Hadzima, Z. Trojanová, P. Lukác, Acta Mater. 54 (2006) 5361–5366.

[18] S. Zheng, Q. Yu, Y. Jiang, Int. J. Fatigue 47 (2013) 174–183.

[19] Y.B. Chun, C.H.J. Davies, Mater. Sci. Eng. A. 528 (2011) 5713–5722.

[20] A. Staroselsky, L. Anand, Int J Plasticity 19 (2003) 1843–1864.

[21] S. Suresh, Fatigue of Materials, Cambridge University Press, 1991.

[22] R. Reed-Hill, W. Robertson, Acta Metall 5 (1957) 728–737.

[23] M. Yoo, Scr. Metall 13 (1979) 131–136.

[24] H. Somekawa, T. Inoue, T. Mukai, Mater. Sci. Eng. A. 527 (2010) 1761–1768.

[25] M. Yoo, Metall Trans. A 12 (1981) 409–418.

[26] J.D. Clayton, J. Knap, Acta Mater. 61 (2013) 5341–5353.

[27] R. Zeng, E. Han, W. Ke, Int. J. Fatigue 36 (2012) 40–46.

[28] A. Berkovits, D. Fang, Eng. Fract. Mech. 51, (1995) 401-416.

[29] V. Moorthy, T. Jayakumar, B. Raj, Mater. Sci. Eng. A. 212 (1996) 273-280.

[30] T. T. Lamark, F. Chmelík, Y. Estrin, P. Lukáč, J. Alloys Compd. 378 (2004) 202–206.

[31] Z. Han, H. Luo, Y. Zhang, J. Cao, Mater. Sci. Eng. A. 559 (2013) 534–542.

[32] A. Vinogradov, A. Lazarev, M. Linderov, A. Weidner, H. Biermann, Acta Mater. 61 (2013) 2434–2449.

[33] T.A. Sisneros, D.W. Brown, B. Clausen, D.C. Donati, S. Kabra, W.R. Blumenthal, S.C. Vogel, Mater. Sci. Eng. A. 527 (2010) 5181–5188.

[34] G. Wan, B.L. Wu, Y.H. Zhao, Y.D. Zhang, C. Esling, Scripta Mater. 65 (2011) 461–464.

Figure captions

Fig. 1 (a) Optical observations of micro-structures, (b) pole figures of (0002), (11-20), and (10-10) for the extruded AZ31 alloy. (c) Details of the CT specimen

Fig. 2 Stress - strain curves during tensile tests for ED and TD specimens

Fig. 3 (a) Crack lengths versus numbers of fatigue cycles, and (b) relationships between crack growth rates and ΔK for different specimens

Fig. 4 Scanning electron micrographs of fracture surfaces for (a) ED and (b) TD specimens at ΔK about 12 MPam$^{1/2}$ (at frequency of 10Hz)

Fig. 5 Optical observations of the cross-sectional micro-structures near fracture surface for

(a, c) ED and (b, d) TD specimens at ΔK about (a, b) 9.25 MPam$^{1/2}$ and (c, d) 16 MPam$^{1/2}$ (at frequency of 2Hz)

Fig. 6 (a) Cumulative AE counts versus fatigue cycles; (b) total AE counts (average of three specimens)

Fig. 7 Relationships between AE count rates and ΔK

Fig. 8 Relationships between AE count rates and FCP rates for different specimens

Fig. 9 Amplitude versus rise time at different ΔK ranges for (a) ED and (b) TD specimens

Fig. 10 Typical waveforms and FFT spectrum for (a) signals with higher RT (>200μs) during fatigue test for TD specimen (b) signals in yielding stage during tensile test for TD specimen (c) signals with lower RT (<200μs) during fatigue test for TD specimen

Fig. 11 Cumulative AE counts for AE events with *RT* <200μs and *RT* >200μs in ED and TD

Fig. 12 Optical observations of the cross-sectional micro-structures near fracture surface for TD specimens at frequency of (a) 2Hz and (b) 20Hz (at ΔK about 16 MPam$^{1/2}$)